Collisionless Absorption in Sharp-Edged Plasmas

Paul Gibbon[a]
Max-Planck-Institut für Biophysikalische Chemie, D-3400 Göttingen-Nikolausberg, Germany

A. R. Bell
The Blackett Laboratory, Imperial College, Prince Consort Road, London SW7 2BZ, England
(Received 2 July 1991)

The absorption of subpicosecond, obliquely incident laser light is studied using a $1\frac{1}{2}$ D particle-in-cell code. Density scale lengths from $L/\lambda=0.01$ to 2 and laser irradiances between $I\lambda^2=10^{14}$ and 10^{18} $\mathrm{W cm^2 \mu m^2}$ are considered. "Vacuum heating" [F. Brunel, Phys. Rev. Lett. **59**, 52 (1987)] dominates over resonance absorption for scale lengths $L/\lambda<0.1$, and is most efficient when $v_{osc}/c\simeq 3.1(L/\lambda)^2$. Absorbed energy is carried mainly by a "superhot" electron population with $U_{hot}\sim(I\lambda^2)^{1/3-1/2}$.

PACS numbers: 52.40.Nk, 52.50.Jm, 52.65.+z

The recent availability of lasers with pulse lengths in the region of 100 fs to 1 ps has enabled target-interaction experiments to be performed for the first time under rather novel conditions [1]. The short duration of the pulse eliminates many of the complications inherent in inertial-confinement-fusion- (ICF-) type laser-plasma interactions. At intensities above 10^{14} $\mathrm{W cm^{-2}}$, the surface of the target will be ionized quickly, but the plasma created will not have time to ablate significantly while the pulse is incident. The small-scale-length plasma thus formed will not support the parametric instabilities which abound in ICF targets.

The interpretation of these experiments has so far been based on collisional models [1–3]. While this approach has produced good agreement at low irradiances ($I\lambda^2<10^{15}$), where the plasma is cool, $T_e\simeq 10$–50 eV, such a description is likely to be inadequate at higher irradiances where collisions cannot account for much of the total absorption. Some alternative candidates identified so far are resonance absorption [4–7], "skin" effects [8–10], and electron heating in the vacuum outside the plasma surface [11].

In this Letter, we attempt to study these collective phenomena under a broad range of density scale length and laser irradiance using particle-in-cell (PIC) simulation. We consider illumination by a single beam only: Studies of "vacuum" heating have been made before assuming geometries of a single pump [7,12] and two oblique, opposing pumps [7,12,13]. While the latter geometry may be suitable for multiple-beam applications (e.g., ICF), the single-pump geometry better describes sub-ps pulses on slab targets. The extensive range of parameters covered here is achieved by means of the following "shortcut."

A simple velocity transformation reduces the usual 2D periodic slab geometry normally required to study resonance absorption to a system with only one spatial dimension, with obvious savings in computational expense. The idea is to use a reference frame in which the electromagnetic wave appears to be normally incident to the target density gradient [14]. Consider a wave $(\omega,\mathbf{k})$, periodic in y, incident on a slab target. Transforming to a frame S' moving with velocity $\mathbf{v}_0=(0,c\sin\theta,0)$ relative to S leads to $\omega'=\omega/\gamma$, $k_y=0$, where $\gamma=(1-v_0^2)^{-1/2}=\sec\theta$. The coordinate y' is therefore ignorable, and the problem is reduced to one spatial (x) and two velocity variables (v_x,v_y). Applying this to a standard $1\frac{1}{2}$ D PIC code, an electromagnetic wave is launched from the left-hand boundary into a thermal plasma streaming perpendicularly at a speed $v_{0y}=c\sin\theta$. It is this drift, via the $v_{0y}B_z$ term in the equation of motion, which produces a force normal to the density gradient, and hence excites electrostatic oscillations in the simulation frame S'. All field and particle quantities are computed in S'; the inverse Lorentz transformation is used to recover the laboratory-frame variables. Owing to our choice of normalization, we keep ω' and k_0' fixed, so care is required in scaling the input parameters with θ. The most important relations are $v_{osc}/c=(v_{osc}/c)'$, where v_{osc} is the quiver velocity in the laboratory-frame electromagnetic (e.m.) wave, $n_e/n_c=\gamma^{-3}(n_e/n_c)'$, and $k_0L=\gamma^{-1}(k_0L)'$. The number of particles used is 16000–32000, and the mesh size is 500–2000 grid points. Absorption is calculated in the usual way from the time-averaged Poynting vector at the left-hand boundary, and from the rate of increase in the total energy of plasma electrons including the kinetic energy of particles leaving the right-hand boundary. About 20 Cray-YMP minutes were required to reproduce one of the 2D results in, for example, Ref. [5]. We note in passing that the above shortcut will only permit parametric processes in which a single electromagnetic k_y is present; sidescatter of the form $k_y\rightarrow k_y'+k_p$ cannot be studied with this technique.

The reader may need convincing that this method really does reproduce the results of a periodic 2D code, so we show an example with parameters similar to one of the simulations performed by Forslund *et al.* [5]. The rms magnetic and electric fields at the end of this run are shown in Fig. 1; these are equivalent to the fields in a 2D code that have been Fourier analyzed in y, apart from the dc and second-harmonic components retained in Fig. 1(b). These plots show excellent quantitative agreement with Ref. [5], apart from a factor of $\sqrt{2}$ owing to the difference in averaging.

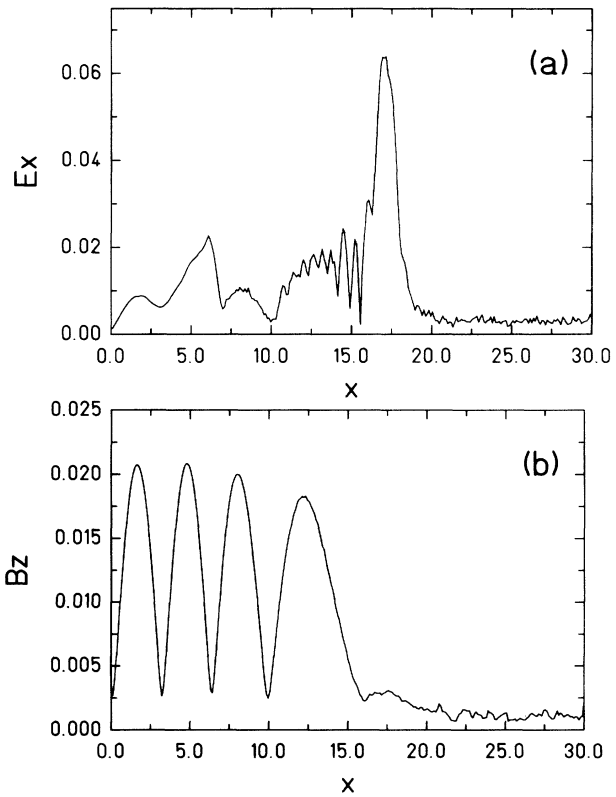

FIG. 1. Average (rms) magnetic and electric fields for $L/\lambda=2$, $v_{osc}/c=0.015$, $\theta=20°$, $n_e/n_c=2$. For this run 32000 particles and 1400 grid points were used.

The classical angular dependence for $L/\lambda \gg 1$ [4,5] is also reproduced; see Fig. 2. As the scale length is reduced, the absorption peaks at larger angles as expected, but the absorbed fraction actually increases, in contrast to the predictions of collisional fluid theory for p-polarized light [15,16]. For $L/\lambda < 0.1$, absorption is dominated by electrons pulled away from the plasma surface and sent back in with velocities $v \sim v_{osc}$, in a manner similar to that described by Brunel [11]. The peak absorption angle of 45° for small scale lengths is consistent with this picture, rather than with one of "modified" resonant absorption. Note that these results do not contradict previous work on resonance absorption [17] in which scale lengths of $L/\lambda < 0.1$ were generated by self-consistent profile steepening, under relatively shallow incidence angles $\theta < 20°$. In the latter simulations, the presence of an extended underdense shelf played a crucial role in supporting a resonant plasma wave. In all cases presented here, however, the density profile used was a simple linear ramp with a vacuum outside the plasma.

The transition from resonant to vacuum heating is illustrated in Fig. 3, which shows shapshots of the electron phase space for $L/\lambda=2$ and 0.2. We notice immediately that the electron orbits for $L/\lambda=0.2$ can be more closely identified with Brunel's model than with the resonant plasma oscillation in Fig. 3(a). Comparing Figs. 3(b)

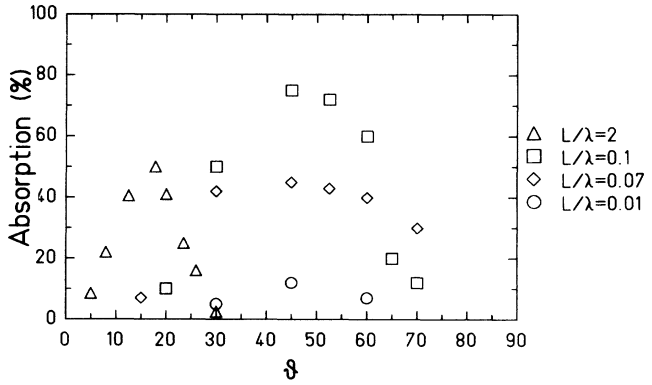

FIG. 2. Absorption vs obliquity for p-polarized light. Density profiles (simple linear ramps) shown are $L/\lambda=2$ (triangles), $L/\lambda=0.1$ (squares), $L/\lambda=0.07$ (diamonds), and $L/\lambda=0.01$ (circles). Parameters common to each case were $I\lambda^2=10^{16}$ W cm^{-2} μm^2, $n/n_c=2$, $T_e=1$ keV.

and 3(d), we observe that whereas resonantly heated electrons pick up a component of the transverse laser momentum, vacuum-heated electrons return to the solid with the same p_y they started with (i.e., mv_{te}). Consequently, in an experiment where the density scale length is changing, one might observe a shift in the direction of the fast electron heat flux.

There are several factors influencing the electron momentum balance normal to the density gradient which are absent in Brunel's simplified model [11]. First, the "capacitor" field is inadequate to describe a *single* oblique electromagnetic wave, which in general comprises both traveling and stationary components: Near the plasma surface electrons will feel a dc force from the radiation pressure. Second, the presence of a small but finite underdense region of plasma allows enough penetration of the e.m. wave to drag electrons out which would otherwise have remained shielded inside a step-profile plasma. Third, not all electrons return to the plasma after every cycle; some remain circulating in the vacuum region, giving rise to an additional dc electric field which tends to prevent further electrons from leaving the plasma. The resulting orbits are therefore more difficult to predict than those in the capacitor approximation.

That there is an interplay of competing effects becomes apparent when we consider the variation of absorption with laser irradiance. As expected, the fractional absorption for "long" scale lengths is almost independent of $I\lambda^2$; see Fig. 4. As L/λ is reduced, however, the intensity dependence becomes characterized by three distinct features: (i) an initial reduction in η when the oscillation amplitudes become larger than the resonance region; (ii) a sharply defined maximum value corresponding to efficient vacuum heating; and (iii) a slow falloff with increasing v_{osc} due to a larger stationary B field at the plasma surface [7,12]. Examination of the peak absorption values indicates that it is most efficient when $v_{osc}/c \simeq 3.1(L/\lambda)^2$. We found no significant dependence on

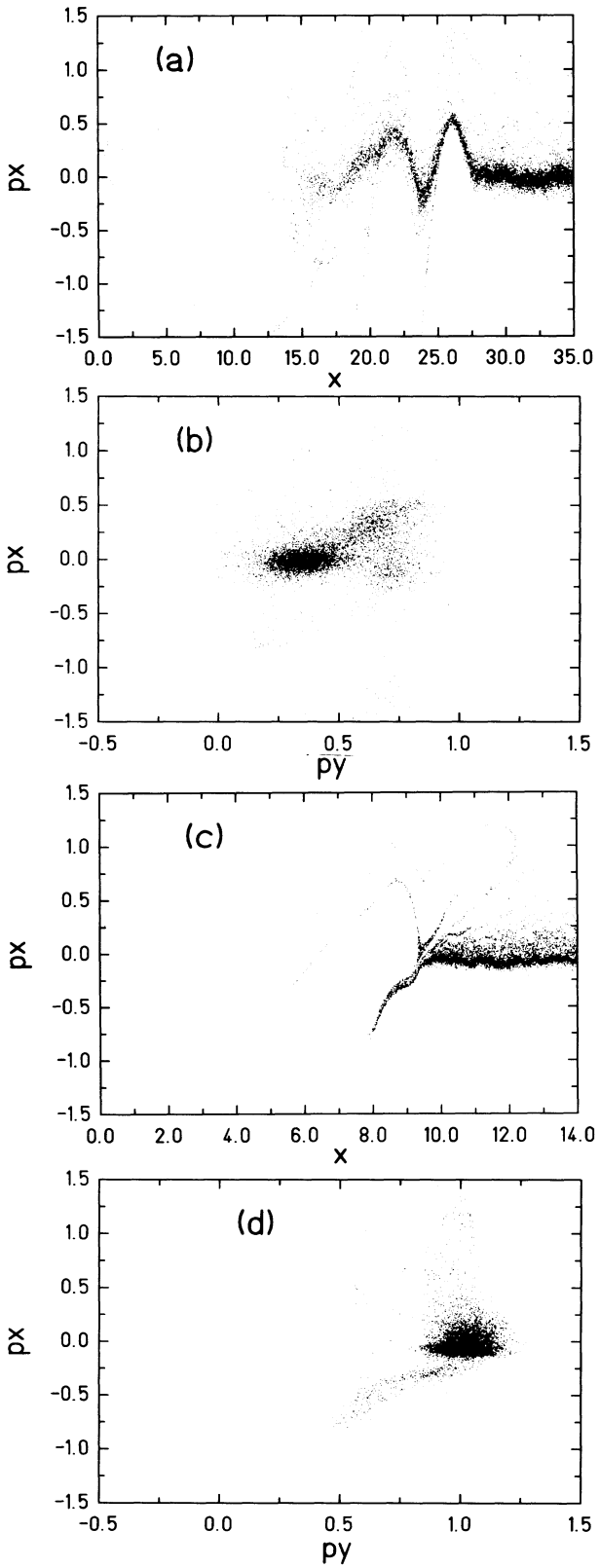

FIG. 3. Electron phase space from two simulations with different density gradients: (a),(b) $L/\lambda=2$, $\theta=23°$; (c),(d) $L/\lambda=0.2$, $\theta=45°$. The other parameters were $I\lambda^2=10^{17}$ W cm^{-2} μm^2, $n/n_c=2$, $T_e=1$ keV.

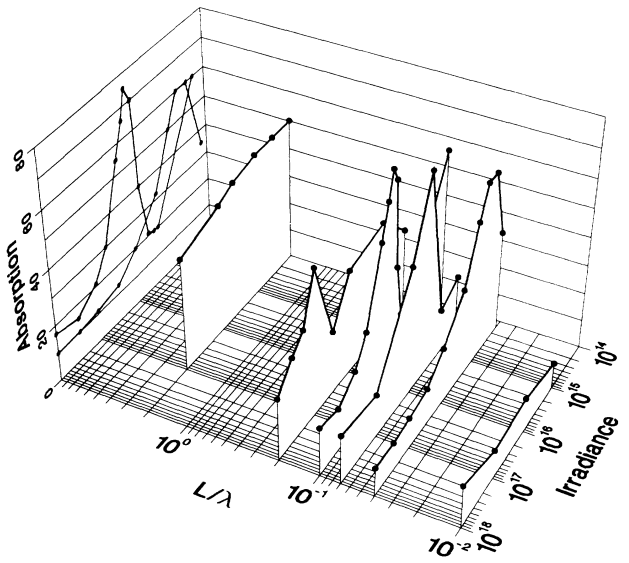

FIG. 4. Absorption percentage in the $I\lambda^2$-L/λ plane for $\theta=45°$. The maximum value is 75% for $L/\lambda=0.1$, $I\lambda^2=10^{16}$. The data for $L/\lambda=0.04$ and 0.1 have been redrawn on the "back wall" for clarity.

background temperature for intensities near and above this optimum, at least for $v_{osc}/v_{te} \gg 1$. Below the optimum, an increase in the Debye length could alter the competition between resonance absorption and vacuum heating, and perhaps affect the above scaling.

For pure step profiles, vacuum heating appears to be negligible; electrons are held inside the plasma and only sample the evanescent part of the e.m. wave. Absorption in this case is due to a form of skin heating (or anomalous skin effect) [18], and is independent of v_{osc} except at very high irradiances, where relativistic effects become important [8,19]. These results are also consistent with

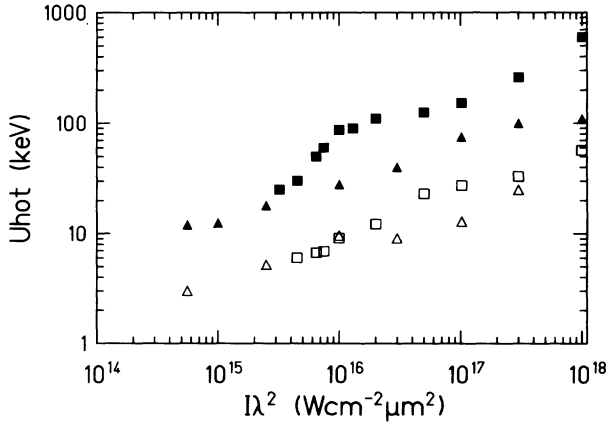

FIG. 5. Energies of escaping electrons (solid symbols) and temperature of hot plasma electrons (open symbols) for $L/\lambda=0.1$ (squares) and $L/\lambda=0.04$ (triangles). The energy of escaping electrons was calculated from the mean of the hot end of the spectrum, which tends to form a beamlike tail rather than a second Maxwellian population.

the step-profile limit cases of Refs. [7,12].

The absorbed energy for $L/\lambda < 0.1$ goes into two kinds of heated electron populations. Inside the plasma a bi-Maxwellian distribution is formed by the electrons heated within the laser penetration depth. No distinction could be made between the small number of resonantly heated electrons and those which just sample the evanescent laser field. Vacuum-heated electrons escape from the high-density boundary with much higher energies $U_{\rm hot} \propto (I\lambda^2)^{1/3-1/2}$; see Fig. 5. The scaling is weaker than that obtained from a capacitor model ($U_{\rm hot} \sim v_{\rm osc}^2$) [11], presumably because the electrons experience deceleration when reentering the underdense plasma [Fig. 3(c)], the magnitude of which increases with intensity.

In conclusion, we have determined the collisionless absorption component of short (p-polarized) laser pulses for a wide range of irradiance and density scale length. "Vacuum heating" is responsible for most of the heating below $L/\lambda = 0.1$, and is most efficient at 45° incidence for an optimum irradiance given by $(v_{\rm osc}/c)_{\rm opt} \propto (L/\lambda)^2$. Comparison with experiments is complicated at present by the fact that collisional absorption will tend to dominate the low-intensity range (of Fig. 4). Another factor is ion motion, which will initially result in a decreasing density gradient [12], but strong steepening towards the center of the pulse. The above scaling for optimal absorption might therefore be exploited by choosing a pulse shape to match the instantaneous L/λ. The technique of "boosted reference frame" presented here can also be used with mobile ions, and would be suitable for extending the study of nonlinear resonance absorption to very long scale lengths (e.g., $L/\lambda \sim 50$) and small angles of incidence ($\theta \sim 5°$).

One of the authors (P.G.) would like to thank P. Mulser for his hospitality at the Institute for Applied Physics, Darmstadt, where part of this work was performed.

[a]Present address: IBM Germany, Wissenschaftliches Zentrum, Tiergartenstrasse 15, 6900 Heidelberg, Germany.

[1] H. M. Milchberg, R. R. Freeman, S. C. Davey, and R. M. More, Phys. Rev. Lett. **61**, 2364 (1988); J. C. Kieffer, P. Audebert, M. Chaker, J. P. Matte, T. W. Johnston, P. Maine, J. Delettrez, D. Strickland, P. Bado, and G. Mourou, Phys. Rev. Lett. **62**, 760 (1989); R. Fedosejevs, R. Ottmann, R. Sigel, G. Kühnle, S. Szatmari, and F. P. Schäfer, Phys. Rev. Lett. **64**, 1250 (1990).

[2] M. Chaker, J. C. Kieffer, J. P. Matte, H. Pépin, P. Audebert, P. Maine, D. Strickland, P. Bado, and G. Mourou, Phys. Fluids B **3**, 167 (1991).

[3] R. M. More, Z. Zinamon, K. H. Warren, R. Falcone, and M. Murnane, J. Phys. (Paris), Colloq. **49**, C7-43 (1988).

[4] V. L. Ginzburg, *The Propagation of Electromagnetic Waves in Plasmas* (Pergamon, New York, 1964), p. 260.

[5] D. W. Forslund, J. M. Kindel, K. Lee, E. L. Lindman, and R. L. Morse, Phys. Rev. A **11**, 679 (1975).

[6] K. G. Estabrook and W. L. Kruer, Phys. Fluids **18**, 1151 (1975).

[7] K. G. Estabrook and W. L. Kruer, in Annual Laser Program Report, Lawrence Livermore National Laboratory, 1986 (unpublished), p. 2-87.

[8] E. G. Gamaliy and R. Dragila, Phys. Rev. A **42**, 929 (1990).

[9] W. Rozmus and V. T. Tikhonchuk, Phys. Rev. A **42**, 7401 (1990).

[10] P. Mulser, S. Pfalzner, and F. Cornolti, in *Laser Interaction with Matter,* edited by G. Velarde, E. Minguez, and J. M. Perlado (World Scientific, Singapore, 1989), p. 142.

[11] F. Brunel, Phys. Rev. Lett. **59**, 52 (1987).

[12] F. Brunel, Phys. Fluids **31**, 2714 (1988).

[13] G. Bonnaud, P. Gibbon, J. Kindel, and E. Williams, Laser Part. Beams **9**, 339 (1991).

[14] A. Bourdier, Phys. Fluids **26**, 1804 (1983).

[15] H. M. Milchberg, R. R. Freeman, S. C. Davey, and R. M. More, Phys. Rev. Lett. **61**, 2364 (1988).

[16] J. C. Kieffer, J. P. Matte, S. Bélair, M. Chaker, P. Audebert, H. Pépin, P. Maine, D. Strickland, P. Bado, and G. Mourou, IEEE J. Quantum Electron. **25**, 2640 (1989).

[17] D. W. Forslund, J. M. Kindel, and K. Lee, Phys. Rev. Lett. **39**, 284 (1977); K. G. Estabrook and W. L. Kruer, Phys. Rev. Lett. **40**, 42 (1978).

[18] E. S. Weibel, Phys. Fluids **10**, 741 (1967).

[19] W. L. Kruer and Kent Estabrook, Phys. Fluids **28**, 430 (1985).

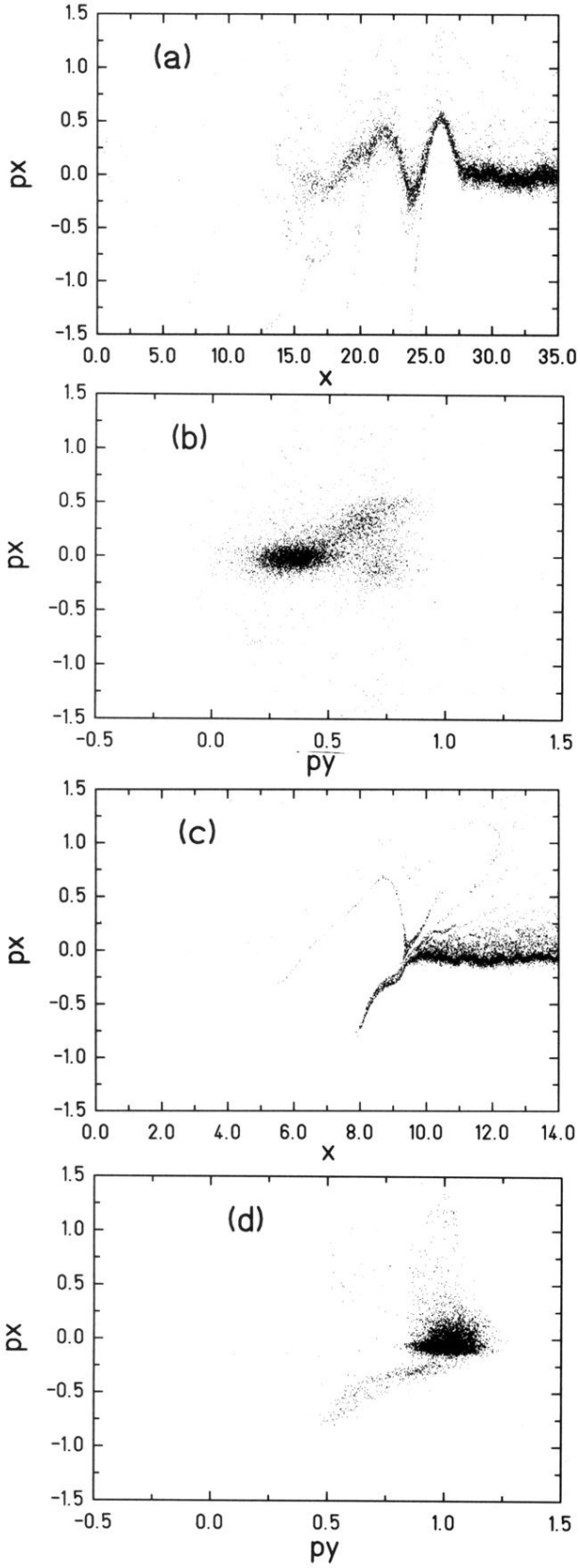

FIG. 3. Electron phase space from two simulations with different density gradients: (a),(b) $L/\lambda=2$, $\theta=23°$; (c),(d) $L/\lambda=0.2$, $\theta=45°$. The other parameters were $I\lambda^2=10^{17}$ W cm^{-2} μm^2, $n/n_c=2$, $T_e=1$ keV.